Graph models of wind instruments : computing the natural frequencies of some elementary ducts

G. Le Vey

Ecole des Mines de Nantes, IRCCyN - UMR CNRS 6597, 4 rue Alfred Kastler, 44300 Nantes, France

georges.le-vey@mines-nantes.fr

A graph-based modelling approach for wind instruments with tone holes has been recently proposed by the author. This preliminary work remained at a rather theoretical level with high degree of generality, focussing nevertheless on musical acoustics applications while laying foundations for concrete applications. The purpose of the present work is to present concrete computation methods and numerical results in order to validate these theoretical results. For this task, elementary resonators are investigated, for which great knowledge has been accumulated for a long time through the impedance, transfer matrix and modal decomposition approaches, which can thus serve for checking. The resonator profiles focussed on belong to a musically useful class : cylinders and stepped cones, as studied by Dalmont and Kergomard 20 years ago. The case of a cylindrical resonator with one tonehole is also presented. One important feature of the approach is that mode matching is automatically satisfied, natural frequencies and eigenmodes being computed at once by the method, even for geometries with discontinuities. Also, perspectives are opened for exhibiting a very wide class of resonators with harmonically related natural frequencies, which is the subject of an another paper.

1   Introduction

The common ways of studying wind instruments are through a modal approach, using the electric-acoustic analogy with equivalent circuits and their impedances within the transmission lines formalism, while approximating a resonator with complex geometry as a sequence of cylinders or cones [1, 2]. In [3], a different modelling approach was presented, based on a 1D-PDE mathematical formalism on networks that has proven useful to other systems [4, 5], made of interconnected elementary components. The basic idea is to consider the graph of this network connecting together the elementary components and to study the eigensolutions of this set through properties of the graph itself and of the components. This allows to keep a one dimensional setting even for complex geometries. A good approximation of the natural frequencies and, at the vertices of the graph, of eigenmodes is obtained in a direct fashion. The presentation is organized as follows : in section 2, the resonators under study are described within the framework of the graph approach [3], briefly reminded in the two appendices. In section 3 natural frequencies computation of several of these resonator profiles is presented and discussed. Conclusions and future research are drawn in section 4.

2   Description of resonators

The study is restricted to elementary wind instruments, within the plane wave hypothesis, in order to validate the approach by checking against results obtained by the usual approaches. Two classes of instruments are investigated here. Firstly, simple resonators with no toneholes but piecewise constant cross-sections : in the sequel, a *n-stepped cone* means such a resonator with n discontinuities in the cross-section. The ones approximating a truncated cone [6] will be especially investigated. Secondly, a mere one tonehole instrument [7]. For each class, the model is given through the matrices $\mathcal{D}, \mathcal{E}, \mathcal{A}, \mathcal{L}$ related to the graph, as summarized in appendix 5.

2.1   Resonators without toneholes

The graph of a piecewise cylindrical resonator without toneholes is a mere sequence of edges with maximum vertex degree two (see the appendix). Thus, instead of writing down explicitly all matrices, we proceed with a notational trick, for saving space and because matrices are tridiagonal (one vertex obviously has only two neighbouring vertices) : diag(v,j) stands for a matrix with jth diagonal ($j \in \mathbb{Z}$)

given by the vector v, and zeroes elsewhere. Such matrices can be added provided convenient dimensions are given. Set U (resp. a, resp. L), the n-vector with all elements equal to one (resp. the cross-sections areas, resp. the lengths) of the edges. Then, a resonator made of n concatenated cylinders with lengths l_i, cross-sections a_i is described by the matrices : $\mathcal{E} = \mathtt{diag(U,-1)+diag(U,1)}$, $\mathcal{D} = \mathtt{diag(-U,0)+diag(U,-1)}, \mathcal{A} = \mathtt{diag(a,-1)+diag(a,1)}$, $\mathcal{L} = \mathtt{diag(L,-1)+diag(L,1)}$ Then, the characteristic matrix $\mathcal{M}(k)$ (see appendix) writes :
$$\mathcal{M}(k) = \mathtt{diag}(\alpha,\mathtt{0})+\mathtt{diag}(\beta,-1)+\mathtt{diag}(\beta,1)$$
with $\alpha = (\alpha_i)_i$, $\beta = (\beta_i)_i$ and : $\alpha_1 = -a_1\frac{c_1}{s_1}$, $\alpha_{n+1} = -a_n\frac{c_n}{s_n}$, $\alpha_i = -(a_{i-1}\frac{c_{i-1}}{s_{i-1}} + a_i\frac{c_i}{s_i}), i = 2,\ldots,n$, $\beta_i = \frac{a_i}{s_i}, i = 1,\ldots,n$ and $c_i = \cos(kl_i)$, $s_i = \sin(kl_i)$. The fact that $\mathcal{M}(k)$ is tridiagonal symmetric allows for fast computations. Needless to say, although the matrix $\mathcal{M}(k)$ is easily constructed, solving the characteristic equation $\det \mathcal{M}(k) = 0$ explicitly by brute force is hopeless as its complexity grows very quickly with the number of cylinders, thus one would have to resort to iterative numerical methods in any case. Instead, it is much more interesting to consider an important special case : when lengths l_i are all equal to the same l the search for natural frequencies reduces to an algebraic eigenvalue problem, for which efficient solvers exist. In that case, let $x = c_i \equiv \cos(kl), y = s_i \equiv \sin(kl)$. Then $\mathcal{M}(k)$ writes :
$$\mathcal{M}(k) = \frac{1}{y}(\mathtt{diag}(\alpha,\mathtt{0})+\mathtt{diag}(\beta,-1)+\mathtt{diag}(\beta,1))$$
with : $\alpha_1 = -a_1 x, \alpha_{n+1} = -a_n x, \alpha_i = -(a_{i-1} + a_i)x, i = 2,\ldots,n, \beta_i = a_i$. One understands that, even for resonators with complex geometries, a sufficiently fine discretization into equal length cylinders allows the above simplification. This is obviously at the price of increasing the dimension of $\mathcal{M}(k)$. But it will be seen that the resulting numerical problem is much more easily amenable to a solution than the nonlinear original one. In the opposite case when not all edge lengths are equal, solving the characteristic equation becomes cumbersome when the number of edges increases.

2.2   Woodwind with one tonehole

In that case, the graph is star-shaped with three edges all connected at one vertex. Choosing the orientation of the three edges for which the origin is at the three simple vertices, the relevant matrices are :

$$\mathcal{D} = \begin{pmatrix} 1 & 0 & 0 & 0 \\ 0 & 1 & 0 & 0 \\ -1 & -1 & -1 & 0 \\ 0 & 0 & 1 & 0 \end{pmatrix}, \mathcal{E} = \begin{pmatrix} 0 & 0 & 1 & 0 \\ 0 & 0 & 1 & 0 \\ 1 & 1 & 0 & 1 \\ 0 & 0 & 1 & 0 \end{pmatrix} \quad (1)$$

with $\mathcal{A}, \mathcal{L}$ having the same pattern and :

$$\mathcal{M}(k) = \begin{pmatrix} -\frac{a_1 c_1}{s_1} & 0 & \frac{a_1}{s_1} & 0 \\ 0 & -\frac{a_2 c_2}{s_2} & \frac{a_2}{s_2} & 0 \\ \frac{a_1}{s_1} & \frac{a_2}{s_2} & -\sum_{i=1}^{3} \frac{a_i c_i}{s_i} & \frac{a_3}{s_3} \\ 0 & 0 & \frac{a_3}{s_3} & -\frac{a_3 c_3}{s_3} \end{pmatrix} \quad (2)$$

and we have corrected a mistake for $\mathcal{M}(k)$ made in [3].

3 Natural frequencies computation

For all numerical computations, the parameters are : $t = 20°C$ for which the sound velocity is $c_0 = 343.37 m/s$. The boundary conditions are given in a simple form by fixing either the pressure (open end) or the volume flow (closed end) to zero. This is done by fixing corresponding values of ϕ_i or $\partial_x \phi_i$ to zero. The notational convention here is to specify the boundary condition for the left end first and then for the right end of the resonator (e.g. open-open or closed-open). The method for computing the natural frequencies is briefly summarized in appendix 5.

3.1 Stepped resonators : formal computations

Consider, as in [6], the case were one end, say the left, is closed and the other end is open. This means that the boundary conditions are fixed as follows : at the left closed end, the potential is not fixed so it has to be computed. At the right open end, it is fixed to vanish (the pressure must vanish). Of course, this is an ideal case and more realistic radiation conditions can be taken into account by fixing a non zero value. The consequence of the vanishing of the potential is that one just has to discard the corresponding columns of $\mathcal{M}(k)$ when solving the algebraic eigenvalue problem, because in that case all the eigenfunctions, hence the eigenvectors of $\mathcal{M}(k)$, vanish at this end. One is thus left with the following characteristic matrix :

$$\mathcal{M}(k) = \frac{1}{y} \begin{pmatrix} \alpha_1 x & \beta_1 & 0 & \cdots & 0 \\ \beta_1 & \alpha_2 x & \beta_2 & \cdots & 0 \\ 0 & \beta_2 & \alpha_3 x & \ddots & 0 \\ \vdots & \ddots & \ddots & \ddots & \vdots \\ 0 & 0 & \cdots & \cdots & \alpha_n x \end{pmatrix} \quad (3)$$

with this time : $\alpha_1 = -a_1$, $\alpha_i = -(a_{i-1} + a_i), i = 2, \ldots, n$, $\beta_i = a_i$. Thanks to its tridiagonal symmetric structure, its determinant $p_n(x)$ is efficiently computed recursively, discarding $y \neq 0$:

$$\begin{cases} p_0(x) & = & 1 \\ p_1(x) & = & \alpha_1 x \\ p_n(x) & = & \alpha_n x p_{n-1}(x) - \beta_{n-1}^2 p_{n-2}(x) , \ n = 2, \ldots, \end{cases} \quad (4)$$

This three terms recursion (4) suggests an interpretation of the family $(p_n(x))_n$ in terms of orthogonal polynomials [8] but this remains to be studied in full generality. Nevertheless, it has the following general property : $\forall k, l \in \mathbb{N}$, d_{2k} is orthogonal to d_{2l+1} on the range $[-1, +1]$ with respect to the weight function : $w(x) = \sqrt{1 - x^2}$, baring similarity with Jacobi polynomials [8]. Such a recursion reminds that found in [6] for the diameters. For the time being, one restricts, as a matter of example, to a special class.

Table 1: $p_n(x), a_n = \frac{n(n+1)}{2} a_1, n = 1, \ldots, 8$

n	$p_n(x)$
1	$-x$
2	$4x^2 - 1$
3	$-x(2x^2 - 1)$
4	$(4x^2 - 2x - 1)(4x^2 + 2x - 1)$
5	$-x(4x^2 - 1)(4x^2 - 3)$
6	$(8x^3 + 4x^2 - 4x - 1)(8x^3 - 4x^2 - 4x + 1)$
7	$-x(2x^2 - 1)(8x^4 - 8x^2 + 1)$
8	$(4x^2 - 1)(8x^3 - x + 1)(8x^3 - x - 1)$

3.1.1 The special progression $a_n = \frac{n(n+1)}{2} a_1$

A whole class of resonators with discontinuities has been shown in [6] to have harmonically related natural frequencies. These resonators are piecewise cylinders such that the sequence of cross-section areas is in the progression $1, 3, 6, \ldots, n(n + 1)/2$. It was conjectured that they should be the only ones with this property. But with the present approach, a wider class is evidenced. (see [9] for some examples). Using recursion (4), Table 1 shows in that particular case the first eight computed $p_n(x)$'s, up to a constant factor that grows rapidly with the degree of $p_n(x)$. One can show that $p_n(x)$ is a particular case of Jacobi polynomial. More precisely, the following identity is true : $p_n(x) = (-1)^n g(n) G_n(x)$ where $G_n(x)$ is the nth ultraspherical (Gegenbauer) polynomial [8] $G(n, a, x)$ with $a = 1$; $g(n)$ is a factor that depends only on n, the degree of the polynomial, and modifies only the normalization of the family. Hence the family $(p_n(x))_n$ is also a polynomial family, that is orthogonal on the interval $[-1, +1]$ with respect to the weight function $w(x) = \sqrt{1 - x^2}$. In this particular case, the zeroes, $\zeta_{k,n}$, of each $p_n(x)$ are those of $G_n(x)$: $\zeta_{k,n} = \cos(\frac{k\pi}{n+1})$, $k = 1, \ldots, n$. One important property evidenced in [6] is thus recovered : for n concatenated cylinders, the partial, which is harmonic, with rank $n + 1$ is missing in the series (look at the zeroes of p_n). Also, for an odd number of cylinders, the natural frequencies of the basic element are also present as one can see on the factorization of p_n in Table 1 (x divides p_n). These two properties are checked on numerical computations below. This explicit knowledge of the solutions to $\det(\mathcal{M}(k)) = 0$ in the particular case of the progression $n(n + 1)/2$ opens interesting perspectives to get deeper insight into both direct and inverse problems related to the natural frequencies of closed-open resonators, as models of reed instruments. This is true as well for other boundary conditions corresponding to different types of wind instruments.

3.2 Numerical results for some stepped cones

As a first example, consider such a piecewise cylindrical resonator with one step only (*1-stepped cone*), where both parts of the resonator have length $0.62m$ and their cross-sections ratio is : $\frac{a_2}{a_1} = 3$. The computed natural frequencies, together with their ratio to the fundamental, appear in Tables 2, 3, 4 respectively for open-open, closed-open, open-closed resonators. In Table 2, one checks that there is a complete harmonic series. In Table 3 (compare with Table 9), notice that the series is now incomplete, all the harmonic multiples of 3 being absent, as foreseen. When the left end is open and the right one is closed (Table 4), the

Table 2: 1-stepped cone, $\frac{a_2}{a_1} = 3$, open-open

Frequency	138.5	276.9	415.4	553.8
f_n/f_1	1	2	3	4
Frequency	692.3	830.7	969.2	1108.0
f_n/f_1	5	6	7	8

Table 3: 1-stepped cone, $\frac{a_2}{a_1} = 3$, closed-open

Frequency	92.3	184.6	369.2	461.5
f_n/f_1	1	2	4	5
Frequency	646.1	738.4	923	1015.3
f_n/f_1	7	8	10	11

Table 4: 1-stepped cone, $\frac{a_2}{a_1} = 3$, open-closed

Frequency	46.2	230.8	323.1	507.7
f_n/f_1	1	5	7	11
Frequency	600	784.6	876.9	1061.5
f_n/f_1	13	17	19	23

Table 5: 2-stepped cone, $\frac{a_2}{a_1} = 3$, $\frac{a_3}{a_1} = 6$, open-open

Frequency	92.3	184.6	276.9	369.2	461.5
f_n/f_1	1	2	3	4	5
Frequency	553.8	646.1	738.4	830.7	923.0
f_n/f_1	6	7	8	9	10

stepped cone is convergent. Then the only harmonics of this resonator are the odd ones, excluding moreover those that are multiples of 3 : this observation seems to be new. Consider now a more complex example. Results for a 2-stepped cone, with length 0.155m each and respective cross-sections 1, 3, 6 are given in Tables 5 and 6. The same conclusions apply : complete series for the open-open case and all multiples of 4 lacking in the series for the closed-open case.

Eventually, as a last example, for the sake of comparison, we did the computations for the closed-open 3-stepped cone example given in [6], p. 427. The computed frequencies appear in Tables 7 to 8. Table 7 is taken from [6] and Table 8 shows the results with our graph-based approach : results in [6] were obtained with a model taking losses into account, which can explain the discrepancies.

3.3 General resonator with one discontinuity

This case is treated e.g. in [10, 2]. The matrix $\mathcal{M}(k)$ writes :

$$\mathcal{M}(k) = \begin{pmatrix} -a_1\frac{c_1}{s_1} & \frac{a_1}{s_1} & 0 \\ \frac{a_1}{s_1} & -(a_1\frac{c_1}{s_1} + a_2\frac{c_2}{s_2}) & \frac{a_2}{s_2} \\ 0 & \frac{a_2}{s_2} & -a_2\frac{c_2}{s_2} \end{pmatrix} \quad (5)$$

Results are given for different boundary conditions. Firstly, when both ends are open (resp. closed), we find that the natural frequencies are the solutions of the equation :
$\frac{a_1}{\tan(kl_1)} + \frac{a_2}{\tan(kl_2)} = 0$ (resp. $\frac{a_1}{\tan(kl_2)} + \frac{a_2}{\tan(kl_1)} = 0$). When the left end is closed and the right end open, the natural frequencies are obtained as those values that make vanish the first principal minor of order two, which is easily shown to be : $-a_1 + a_2\frac{c_1}{s_1}\frac{c_2}{s_2}$. And its solutions are those of the transcendental equation : $\tan(kl_1)\tan(kl_2) = \frac{a_2}{a_1}$. One recognizes this well-known equation (eq. (7.19), p. 259 in [2] e.g.). Exchanging closed and open ends, the natural frequencies are the solution of : $\tan(kl_1)\tan(kl_2) = \frac{a_1}{a_2}$. Notice the symmetry between both equations. Instead of solving these nonlinear equations as usual, here one discretizes the two cylinders in small parts of equal length, and then solves a suitable algebraic eigenvalue problem. As an example, consider such a resonator where both cylinders have length 0.62m and their cross-sections ratio is : $\frac{a_2}{a_1} = 2$. Table 9 shows the results for the open-open (resp. closed-open) case. No special relationship between natural frequencies appears in this case. Notice also that when both ends are either open or closed, one has harmonic frequencies, whatever a_1, a_2, because then, the equation to be solved is reduced to : $\frac{a_1+a_2}{\tan(kl)} = 0$, i.e one has always $kl = \frac{\pi}{2} + l\pi, l \in \mathbb{Z}$.

3.4 General resonator with two discontinuities

Computing the natural frequencies is still an easy matter. In that case, the characteristic matrix $\mathcal{M}(k)$ is :

$$\begin{pmatrix} -a_1\frac{c_1}{s_1} & \frac{a_1}{s_1} & 0 & 0 \\ \frac{a_1}{s_1} & -(a_1\frac{c_1}{s_1} + a_2\frac{c_2}{s_2}) & \frac{a_2}{s_2} & 0 \\ 0 & \frac{a_2}{s_2} & -(a_2\frac{c_2}{s_2} + a_3\frac{c_3}{s_3}) & \frac{a_3}{s_3} \\ 0 & 0 & \frac{a_3}{s_3} & -a_3\frac{c_3}{s_3} \end{pmatrix} \quad (6)$$

from which one obtains the natural frequencies of the closed-closed case e.g. as the solutions of :
$\frac{a_1}{\tan(kl_2)\tan(kl_3)} + \frac{a_2}{\tan(kl_3)\tan(kl_1)} + \frac{a_3}{\tan(kl_1)\tan(kl_2)} = \frac{a_1 a_3}{a_2}$.
We are not aware of such an equation before. Nevertheless, solving this equation for k would be very difficult. Needless to say, in the case of more than two discontinuities, one can compute the determinant of $\mathcal{M}(k)$ thanks to a symbolic computation system but get a complex and long expression that even can hardly be written down. Computing its roots becomes quickly a task out of reach, except when all lengths l_i are equal to l. In that case, the natural frequencies are easily computed through the corresponding algebraic eigenvalue problem, as in 3.3, or through the recursion (4). For the closed-closed case they are given as : $\tan^2(kl) = \frac{a_2(a_1+a_2+a_3)}{a_1 a_3}$. For the closed-open case they are are found through the recursion (4) to satisfy : $\tan^2(kl) = \frac{a_2 a_3}{a_1 a_2 + a_1 a_3 + a_2^2}$. These simple relations already show that several configurations with three cylinders may lead to harmonic natural frequencies. It is obvious that the first relation is invariant under permuting a_1 and a_3, implying several different waveguides. Such symmetry properties are currently under study.

3.5 Resonator with one tonehole

$\mathcal{M}(k)$ is given in (2). It is symmetric but not tridiagonal and the natural frequencies when all external vertices are either open or closed are again the solutions of $\det \mathcal{M}(k) = 0$:
$\frac{a_1}{\tan(kl_2)\tan(kl_3)} + \frac{a_2}{\tan(kl_3)\tan(kl_1)} + \frac{a_3}{\tan(kl_1)\tan(kl_2)} = 0$
where one recognizes the left member of equation for the 3-stepped cone of section 3.4. We have not investigated that point at the moment. Similar relations can be found easily for different configurations of the tonehole and/or the right end, allowing to revisit this subject. As for the equation in section 3.4, it would be very difficult, if not impossible, to solve in full generality such an equation, except maybe in the low frequency approximation, which we did not try yet but will be investigated later. Instead here, one uses the same method as above, discretizing the different parts of the instrument in order to get equal lengths cylinders and solve

Table 6: 2-stepped cone, $\frac{a_2}{a_1} = 3$, $\frac{a_3}{a_1} = 6$, closed-open

Frequency	69.2	138.5	207.7	346.1	415.4
f_n/f_1	1	2	3	5	6
Frequency	484.6	623.0	692.3	761.5	900.0
f_n/f_1	7	9	10	11	13

Table 7: Closed-open 3-stepped cone, results from [6]

Frequency	211.7	429.8	645.8	863.3
f_n/f_1	1	2.03	3.05	4.08

Table 8: Closed-open 3-stepped cone, graph method

Frequency	221.5	443.1	664.6	886.1
f_n/f_1	1	2	3	4

Table 9: 1-stepped cone, $\frac{a_2}{a_1} = 2$, closed-open

Frequency	80.7	185.3	290.5	395.8
f_n/f_1	1	2.29	3.60	4.90
Frequency	501.1	606.5	711.9	817.2
f_n/f_1	6.21	7.51	8.82	10.12

the associated algebraic eigenvalue problem. As a simple illustration, one has computed natural frequencies for the following data : the main resonator is closed-closed, made of two cylinders, each with length $l_1 = 0.62m$ and cross-section area a_1 taken for unit. The tonehole is placed exactly at the middle of the main resonator. It has length $l_2 = 0.155m$ and cross-section area a_2 such that the ratio $\frac{a_2}{a_1}$ grows from 10^{-4} to 1 by steps of 0.1. The evolution of natural frequencies appear in Table 10 (resp. 11) when the tonehole is open (resp. closed). The first four partials are shown in each case, in order to see the evolution in low and somewhat higher frequencies, as a function of the tonehole size. When the tonehole is open, one sees a very low frequency appear, far below the first partial $f_1 = 138.45Hz$ (see the discussion in [2], p. 259), and increasing with increasing cross-section of the hole, while almost not perturbing the other natural frequencies, except when a_2 comes close to a_1. When the hole is closed this very low frequency is absent and the other natural frequencies are much less perturbed by the tonehole volume, which is as to be foreseen. When the tonehole is open (resp. closed) f_3 (resp. f_2) is recognized to be a partial of one open-open cylinder alone, $c/2L$, which is justified theoretically [5].

4 Conclusion and future research

In this work, computation of natural frequencies of wind instruments, for several resonator geometries with and without tonehole or with discontinuities has shown the efficiency of the graph-based approach. The main reason is that computations are done through the solution of an algebraic eigenvalue problem, instead of iteratively solving a nonlinear equation (possibly through optimization) that becomes quickly very complex with the usual approach. Solutions for resonators with discontinuities are computed at no supplementary cost, either theoretical or computational, than without them : the eigenmodes (more precisely their value at the vertices of the graph) are computed at once with natural frequencies, through solving the characteristic equation. Mode matching is automatically satisfied by construction (boundary condition in equation (7) expresses volume flow conservation from start). This can be compared to the approach in [7] (see also [2], chap. 7), where modal decompositions of each branching tube has to be done followed by mode matching. No theoretical developments beyond those summarized in the appendix are needed. All the computed quantities are exact, up to the numerical precision and, of course, *within the plane wave hypothesis* ; for example the familiar notion of length correction, related

to deviation from ideal geometries, is never used, as one has noticed. This has to be compared with the classical modal decomposition, that appears more involved at both levels. The price to pay is to get familiar with the basic mathematical language of graphs, which is likely not in use in the acoustics community. But the procedure can be automatized easily, the only quantities to manipulate being the incidence and adjency matrices and matrices with the same pattern. On another hand, the usual approaches through impedances, transfer matrices and modal decompositions are more appealing to intuition, in part probably because of history, so that both approaches are surely useful for the study of wind instruments. Several other elementary resonators have been studied with this graph approach such as expansion chambers or stepped cones with one tonehole, or even general tree-like resonators, but have not been presented because room is lacking. Nevertheless, refer to [9] for a sample of current developments relying on the present approach, that show that the class of resonators with harmonically related frequencies is much wider than conjectured in [6]. Several directions will be now investigated : characterization of the class of resonators with harmonically related natural frequencies ; investigation of the orthogonal polynomial property ; extension to conical elements, for a better approximation of flaring horns and other variable cross-section resonators, still in the 1D situation ; junction models more general than Kirchoff laws. On another side 2D models, including losses, and other applications to general acoustical problems, including planar and 3D networks of waveguides, are also being considered along the same line.

5 Appendix

Graph description of a wind instrument   The description of a wind instrument by its graph was given in [3], following [5]. A quick summary is given here. Each portion of the main resonator between two adjacent toneholes is modelled in a schematic way by an edge with two ends modelled by two vertices (figure 1). Each tonehole or register hole is modelled schematically as an edge joining two vertices. For piecewise cylindrical resonators, each piece is modelled by an edge joining two vertices that connect it to its two neighbouring cylinders. Then the union of all these edges and vertices constitutes the graph of the wind instrument, which actually is a tree, as illustrated in figure 1 : for a wind instrument with n holes (tone and register holes), the associated tree has $N = 2n + 2$ vertices (or nodes), denoted V_i, and $N - 1 = 2n + 1$ edges, denoted

Table 10: Closed-closed resonator, one open tonehole

a_2/a_1	10^{-4}	10^{-3}	10^{-2}	10^{-1}	1
f_4	415.37	415.37	415.45	416.26	423.09
f_3	276.91	276.91	276.91	276.91	276.91
f_2	138.46	138.51	138.99	143.84	184.61
f_1	1.25	3.94	12.39	37.13	77.85

Table 11: Closed-closed resonator, one closed tonehole

a_2/a_1	10^{-4}	10^{-3}	10^{-2}	10^{-1}	1
f_3	415.36	415.31	414.83	409.98	369.21
f_2	276.91	276.91	276.91	276.91	276.91
f_1	138.45	138.45	138.36	137.56	130.73

E_i. Each edge and its associated quantities are indexed by an integer : $i \in \mathcal{I} = \{1, \ldots, N-1\}$. Therefore, one defines for each edge, the length l_i, the running variable $x_i \in [0, l_i]$, the cross-section area a_i, the pressure p_i, the particle velocity v_i and the velocity potential ϕ_i ($v_i = \partial_{x_i}\phi_i$), $i \in \mathcal{I}$. The sound velocity, c, is assumed to be constant and identical for all resonators. The locations of end points of each tube, i.e. the vertices of the tree, are labelled by $j \in \mathcal{J} = \{1, \ldots N\}$. For $j \in \mathcal{J}$, it is useful to define : $\mathcal{I}_j = \{i \in \mathcal{I} :$ the ith tube meets the jth vertex$\}$ The *incidence matrix* is : $\mathcal{D} = (d_{ij})$, $d_{ij} = 1$ (resp. $d_{ij} = -1$) if the end (resp. the origin) of E_j is V_i, $d_{ij} = 0$ else. The *adjacency matrix* is $\mathcal{E} = (e_{ij})$, $e_{ij} = 1$ if V_iV_j is an edge, $e_{ij} = 0$ else. It describes how edges connect vertices. Denote by $s(i, j)$ the number of the edge connecting vertices V_i and V_j. Whenever $e_{ij} = 0$, set $s(i, j) = 1$. Define then the matrices : $\mathcal{A} = (a_{ih}) = (a_{s(i,h)}e_{ih})$, $\mathcal{L} = (l_{ih}) = (l_{s(i,h)}e_{ih})$, having the same pattern as $\mathcal{E}$ and holding respectively the areas and lengths information. An element by element matrix calculus, named after J. Hadamard, is also needed (see [3]) : $(P \star Q)_{ij} = p_{ij}q_{ij}$, $(M^{(k)})_{ij} = m_{ij}^k$. A star is used to distinguish Hadamard matrix product from the usual one. Set $e = (1, \ldots, 1)^T$ and, for any n-vector, $y = (y_i)$ the diagonal matrix diag(y)= $(\delta_{ij}y_i)$ with δ the Kronecker delta function. The rescaling onto the unit interval $[0, 1]$ is done by setting $x_j = l_jx$, as follows. For the unknown velocity potential $\phi : \mathbf{G} \rightarrow \mathbb{R}$ ($\phi = (\phi_i)_{i\in\mathcal{I}}$) and $x \in [0, 1]$, define the matrix of rescaled unknowns $\Phi(x) = (\phi_{ih}(x))$ with : $\phi_{ih}(x) = e_{ih}\phi_{s(i,h)}\left[l_{ih}\left(\frac{1+d_{is(i,h)}}{2} - xd_{is(i,h)}\right)\right]$ such that : $\Phi(0) = \left(\phi_i(x_{ij}, t)\right)e^T \star \mathcal{E} = \psi e^T \star \mathcal{E}$. $\psi = (\phi_i(x_{ij}, t))$ denotes the vector of values of ϕ_i's at the vertices, with $x_{ij} = 0$ or l_i corresponding to which end meets the other tubes at the jth vertex. Notice the symmetry $\phi_{hi}(x) = \phi_{ih}(1-x)$, $x \in [0, 1]$. As the independent variables x_i have all been rescaled to $[0, 1]$, the spatial derivatives are denoted in the usual way : $u' = \partial_x u$.

Computing the natural frequencies through the graph
Refering to [3], the natural frequencies of a wind instrument model are given as $k = \frac{\omega}{c}$, the wave number, solution of the following eigenvalue problem :

$$\begin{cases} \phi_{ih} \in C^2([0, 1]) \text{ and } (e_{ih} = 0 \Rightarrow \phi_{ih} = 0) \forall i, h \in \mathcal{I} \\ \mathcal{L}^{(-2)} \star \Phi''(x) = -\frac{\omega^2}{c^2}\Phi(x), \forall x \in [0, 1] \\ \exists \psi \in \mathbb{R}^N : \Phi(0) = \psi e^T.\mathcal{E} \\ \left[\mathcal{L}^{(-1)} \star \mathcal{A} \star \Phi'(0)\right]e = 0 \\ \Phi^T(x) = \Phi(1-x), \forall x \in [0, 1] \end{cases} \quad (7)$$
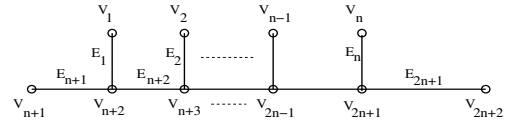

Figure 1: Graph of a wind instrument with n toneholes

Using the Hadamard calculus above, the solution Φ of this problem is : $\Phi(x) = \cos(k\mathcal{L}x)\star\Phi(0)+\frac{1}{k}\mathcal{L}^{-1}\star\sin(k\mathcal{L}x)\star\Phi'(0)$ assuming ω can be computed. Define the matrix : $\mathcal{M}(k) = \mathcal{A} \star (\sin(k\mathcal{L}))^{-1} - \text{diag}\left[\left(\mathcal{A} \star (\sin(k\mathcal{L}))^{-1} \star \cos(k\mathcal{L})\right)e\right]$. The eigenvalues of problem (7) can be shown to be the solutions of the transcental equation : $\det \mathcal{M}(k) = 0$. When all lengths of individual edges of the graph are equal to a given length l, the natural frequencies are merely the solutions of the following algebraic eigenvalue problem (see [3, 5]) : $\mathcal{A}\psi = \cos(kl)\text{diag}(\mathcal{A}e)\psi$. , i.e. defining the matrix $Z := (\text{diag}(\mathcal{A}e))^{-1}\mathcal{A}$ and $\mu = \cos(kl)$: those of the problem : $Z\psi = \mu\psi$. and one sees that the values of the eigenvectors at all nodes are readily computed at once.

References

[1] N. Fletcher and T. Rossing, *The physics of musical instruments*. Springer, 1991.

[2] A. Chaigne and J. Kergomard, *Acoustique des instruments de musique*. Belin, 2008.

[3] G. Le Vey, "Graph-based models for woodwinds," in *SMAC2013, Stockholm Music Acoustics Conference*, Stockholm, July 2013.

[4] S. Nicaise, "Some results on spectral theory over networks applied to nerve impulse transmission," in *Lecture notes in mathematics*, C. Brezinski, Ed., 1985, pp. 533–541.

[5] J. Von Below, "A characteristic equation associated to an eigenvalue problem on c^2 networks," *Linear algebra and its applications*, vol. 71, pp. 309–325, 1985.

[6] J. P. Dalmont and J. Kergomard, "Lattices of sound tubes with harmonically related eigenfrequencies," *Acta Acustica*, vol. 2, no. 5, pp. 421–430, 1994.

[7] V. Dubos, J. Kergomard, A. Khettabi, J. P. Dalmont, D. H. Keefe, and C. J. Nederveen, "Theory of sound propagation in a duct with a branched tube using modal decomposition," *Acta Acustica*, vol. 85, pp. 153–169, 1999.

[8] G. Szegö, *Orthogonal polynomials*, 4th ed., ser. Colloquium publications. Providence, R.I. (1939): American Mathematical Society, 1975, vol. XXIII.

[9] J. P. Dalmont and G. Le Vey, "New lattices of sound tubes with harmonically related eigenfrequencies," in *International Symposium on Musical Acoustics, ISMA'2014*, Le Mans, France, 2014.

[10] J. Kergomard and A. Garcia, "Simple discontinuities in acoustic waveguides at low frequencies : critical analysis and formulae," *J. Sound and Vibration*, vol. 114, no. 3, pp. 465–479, 1987.